THE ASTROPHYSICAL JOURNAL, 408:452–459, 1993 May 10

A SPECTRAL STUDY OF FOUR X-RAY–SELECTED BL LACERTAE OBJECTS WITH *EXOSAT*

R. M. SAMBRUNA,[1] P. BARR,[2] L. MARASCHI,[3] G. TAGLIAFERRI,[2,4] AND A. TREVES[1]

Received 1992 August 20; accepted 1992 October 16

ABSTRACT

We present new *EXOSAT* spectral results for four X-ray–selected BL Lac objects (H0323+022, H0414+009, H1426+428, and H1722+119). The data were retrieved from the *EXOSAT* data base. A spectral analysis was performed on the overall low-energy plus medium-energy distributions, which were modeled with a single, absorbed power law. In one case (H1426+428), an indication of a spectral break at ~5 keV is found. For H0323+022 and H0414+428, for which more than one observation is available, the spectral index is found to vary with intensity, in the sense of a hardening of the spectrum when the source brightens.

Subject headings: BL Lacertae objects: general — X-rays: galaxies

1. INTRODUCTION

Our knowledge of the spectral properties of BL Lac objects in the X-ray band is still rather limited. A number of individual objects have been studied with various satellites (Madejski 1985; Urry 1986; Maraschi & Maccagni 1988 and references therein). A systematic analysis of the data gathered with the *Einstein* Imaging Proportional Counter (IPC) (0.2–2.4 keV) was performed by Worrall & Wilkes (1990). Due to the limited energy range and resolution of these detectors, however, only power-law fits could be considered. From a comparison of the IPC and Monitor Proportional Counter (MPC) data, Madejski & Schwartz (1989) found "statistical" evidence, in six objects, of a systematic steepening of the spectra above 1–3 keV.

The *EXOSAT* satellite instrumentation, involving a low-energy (LE) telescope and a medium-energy (ME) proportional counter, has an effective energy range of almost two decades (0.1–10 keV) and is therefore well suited for broad-band spectral analysis. The studies of individual objects are reviewed in Maraschi & Maccagni (1988). Barr et al. (1989), on the basis of a homogeneous analysis for 17 objects, showed that a broken power law is required to fit the "cumulative" spectral data for this sample. Giommi et al. (1990) studied the ME/LE hardness ratios for a sample of 36 objects, including those reported here, and found indications that the spectrum becomes harder when the source brightens.

Here we present the spectral analysis of the *EXOSAT* data of four BL Lac objects for which individual spectral fits have not been previously published. The aim of this work is to derive individual spectral parameters and to study in more detail the "spectral curvature" inferred from the global sample. This paper is a part of a wider program, still in progress, to systematically reanalyze the archival *EXOSAT* spectra of a larger sample of BL Lac objects.

We structure the paper as follows. In § 2 we describe briefly the discovery, identification, and previous X-ray observations of the target objects. In § 3.1 the *EXOSAT* data are described, together with the criteria employed in selecting the spectra from the data base. In § 4 we give the results of the spectral analysis, while in § 5 we report the results for the individual objects compared with the findings of previous missions. Finally, discussion and conclusions are given in § 6.

2. THE TARGET OBJECTS

The objects considered here, H0323+022, H0414+009, H1426+428, and H1722+119, were all discovered by X-ray experiments operating in the medium-energy band, 2–6 keV, and were later identified as BL Lac objects. The relevant information and references are summarized in Table 1. In column (1) we list the target objects; in columns (2) and (3) we give the references concerning their discovery and the identification, respectively. The redshifts, when available, are given in column (4), with references in parentheses. Columns (5)–(8) are a summary of the X-ray spectral information available from missions other than *EXOSAT*. The data were well fitted, in all reported cases, by a power-law model with photon index α and absorption parameterized in terms of the column density, N_H, in units of 10^{20} cm^{-2}. The references for the previous X-ray analyses are listed in column (9). Note that while some spectral information is available for H0323+022 and H01414+009, very little is known about H1426+428 and H1722+119.

3. *EXOSAT* OBSERVATIONS

3.1. *The Medium-Energy Data*

The ME (Turner, Smith, & Zimmermann 1981) experiment consisted of eight argon-filled proportional counters, sensitive in the 1–20 keV energy range. They were grouped to form two panels ("halves"). During the observations, one half was pointing toward the source ("aligned half"), while the other monitored the sky ("offset half"), giving an independent background estimate. Normally during the observation the two halves were interchanged ("array swap"), to provide a better background determination.

The archival ME data were originally reduced by the automatic analysis described in the *EXOSAT* Database System (1991) manual. The quality of the products relies critically on the way in which the background is obtained. The best results are obtained in the case of the array swaps, because the background is estimated by the same detectors at different times.

As a measure of the reliability of the background subtraction, the extracted spectra were subsequently flagged with a number ranging from 0 to 5. In general, only spectra flagged

[1] SISSA/ISAS, Strada Costiera 11, 34014 Trieste, Italy.
[2] *EXOSAT* Observatory, European Space Agency, ESTEC, Postbus 229, 2200 AG Noordwijk, The Netherlands.
[3] Dipartimento di Fisica, via Dodecaneso 33, 16146 Genova, Italy.
[4] Postal address: Osservatorio Astronomico di Brera, via Brera 28, I-20121 Milano, Italy.

TABLE 1

HISTORY TABLE

Object (1)	Discovery References (2)	Identification References (3)	z (4)	X-Ray Spectral Information for Other Missions: *Einstein* IPC (0.2–4.0 keV) α (5)	*Einstein* IPC (0.2–4.0 keV) N_H (10^{20} cm^{-2}) (6)	*Einstein* MPC (1.2–10 keV) α (7)	*Ginga* (2–35 keV) α (8)	Spectral Information References (9)
H0323+022.....	1, 2	7	0.147 (8)	2.4 ± 0.2	14^{+7}_{-5}	2.8 ± 0.3	2.9 ± 0.2[a] 2.1 ± 0.1[a]	7, 10
H0414+009.....	3	3	0.287 (9)	$2.6^{+0.5}_{-0.4}$[b]	35^{+18}_{-14}[b]	[b]	...	9
H1426+428[c].....	4	4	0.129 (4)	...	...	...	...	
H1722+119.....	5, 6	5, 6	...	...	...	2.7 ± 0.7	...	6

Col. (1).—Object name.
Cols. (2) and (3).—Discovery and identification references, respectively.
Col. (4).—Redshift with reference given in parentheses.
Cols. (5)–(8).—X-ray spectral information obtained from other missions. Cols. (5) and (6) give the spectral index and absorption, respectively, for the *Einstein* IPC; col. (7) gives the spectral index for the *Einstein* MPC; and col. (8) gives the spectral index for *Ginga*.
Col. (9).—References for the spectral information given in the preceding four columns.

[a] The flux increased by a factor of 3 from the steeper to the flatter state in ~5 hr.
[b] From a joint fit to the IPC + MPC.
[c] *ROSAT* and BBXRT data are available for H1426; see text.

REFERENCES.—(1) Doxsey et al. 1983; (2) Piccinotti et al. 1982; (3) Ulmer et al. 1983; (4) Remillard et al. 1989; (5) Griffiths et al. 1989; (6) Brissenden et al. 1990; (7) Feigelson et al. 1986; (8) Filippenko et al. 1986; (9) Halpern et al. 1991; (10) Ohashi 1989.

3–5 can be used for spectral analysis purposes. In some cases, however, it is possible to improve the quality of a spectrum with flag less than 3 by going back to the original tape and performing a more complex reextraction analysis.

We proceeded in the following way to select the data. For a given object, we considered first, for each observing epoch, the ME count rates provided by the automatic analysis in the 1–8 keV energy range. We discarded observations for which the significance of detection was less than a given threshold, which we fixed at 5 σ. The observations flagged 3 or above were retrieved from the data base. To control the quality of the extracted signal, we plotted the spectrum in counts cm^{-2} s^{-1} channel^{-1}, and we looked at the corresponding background light curve and at the LE images to check for contaminating sources. The observations with significance at 5 σ but flagged less than 3 were reextracted, obtaining improved results. The reextraction was performed using the VAX HP software implemented at ESTEC. Observations selected according to the above method are listed in Table 2 (col. [2]). Observations for which a reextraction has been performed are marked. We

TABLE 2

SUMMARY OF *EXOSAT* OBSERVATIONS

Object (1)	Date (2)	LE Exposure Time (s) (3)	LE Count Rate ($\times 10^{-2}$ counts s^{-1}) (4)	ME Exposure Time (s) (5)	ME Count Rate[a] (counts s^{-1}) (6)
H0323+022.....	1984 Sep 21[b]	3423	3.2 ± 0.4 3LX	21490	0.77 ± 0.04
		3610	2.8 ± 0.4 AP		
		11046	0.7 ± 0.1 BO		
	1984 Sep 23[b]	13218	2.8 ± 0.2 3LX	19270	1.14 ± 0.12
H0414+009.....	1984 Sep 9	2635	3.5 ± 0.5 3LX	13820	1.94 ± 0.05
		3779	2.3 ± 0.3 AP		
		4829	1.2 ± 0.2 BO		
	1984 Sep 14	4293	3.7 ± 0.4 3LX	14190	2.30 ± 0.05
		6652	2.6 ± 0.3 AP		
	1984 Sep 22[b]	2643	3.7 ± 0.5 3LX	12790	1.42 ± 0.05
		7091	2.1 ± 0.2 AP		
	1984 Sep 30	3440	3.8 ± 0.4 3LX	10260	1.14 ± 0.05
		4153	2.4 ± 0.3 AP		
		2004	0.6 ± 0.2 BO		
H1426+428.....	1985 Jan 12	5741	32.7 ± 0.8 3LX	7940	4.21 ± 0.07
	1985 Feb 24[b]	3934	28.7 ± 1.2 3LX	46320	3.14 ± 0.06
		1308	11.6 ± 1.1 AP		
		6825	2.4 ± 0.2 BO		
H1722+119.....	1985 Sep 3	5243	2.5 ± 0.3 3LX	20110	0.75 ± 0.04
		5549	1.7 ± 0.2 AP		
		5665	0.4 ± 0.1 BO		

[a] In the energy range 1–8 keV.
[b] Reextracted spectrum (see text).

report the exposure times in column (5). Column (6) gives the count rates in the 1–8 keV energy range.

3.2. *The Low-Energy Data*

The low-energy imaging telescope (de Korte et al. 1981) operated in the soft X-ray band (0.04–2.0 keV). A photon-counting Channel Multiplier Array (CMA), without intrinsic energy resolution, was located in the focal plane. Of the five available filters (offering broad-band spectral resolution), only thin Lexan (Lexan 3000 Å), aluminum-parylene (AP), and boron (Bo) were used for the observations reported here.

In Table 2 we report the intensity of the sources in the various filters and the corresponding exposure times (cols. [4] and [3], respectively). Only the observing dates for which an acceptable ME spectrum could be obtained (see above) are listed (col. [2]). The corresponding LE images in all filters were taken from the CMA data base and were analyzed using the X-ray image analysis package XIMAGE (Giommi & Tagliaferri 1991). We extracted the count rates in a box centered on the source position and with a size which optimizes the signal-to-noise ratio (using the program SOSTA; Giommi & Tagliaferri 1991). The background was estimated in a rectangular region around the source.

4. DATA ANALYSIS AND RESULTS

Spectral analysis of the data was performed using the XSPEC fitting program (Shafer et al. 1991). A number of trial models, folded with the instrumental responses, were compared with the data; the best-fitting parameters were obtained by minimizing χ^2. Besides the ME spectra, we also considered the overall LE + ME energy distributions, obtained by adding the LE data points from the various filters to the ME spectra. Both distributions were studied first using an absorbed power-law model of the form $dN/dE \propto \exp[-N_H \sigma(E)]E^{-\alpha}$ photons cm^{-2} s^{-1} keV^{-1}, with the cross section $\sigma(E)$ taken from Morrison & McCammon (1983), and with the absorption column density N_H in cm^{-2}. Two models have been fitted. In model *a*, N_H was fixed to the Galactic value; in model *b*, N_H was allowed to vary. In Table 3 we list the results from the fits to the ME data with model *a* and to the LE + ME data with both models *a* and *b*. The Galactic values for N_H, also listed in Table 3, are taken from the *EXOSAT* data base, and correspond to the interpolation of the values in the H I map of the Galaxy (Stark et al. 1992). Errors on the quoted Galactic absorbing columns are typically of the order of $\sim 10^{19}$ cm^{-2} (Elvis, Lochmann, & Wilkes 1989). The errors in Table 3 for the spectral parameters are 90% confidence limits for model *a* and 68% confidence limits for model *b*. Column (2) of Table 3 gives the fluxes in the 2–6 keV energy range, corrected for absorption. We plot the spectra, folded with the power-law model, and their corresponding residuals in Figures 1–9 (*upper and lower panels, respectively*).

In some cases the power-law model did not give completely acceptable results (see below). Since, in previous works, a two component X-ray continuum has been proposed for BL Lac objects (Barr, Giommi, & Maccagni 1988; Barr et al. 1989; Madejski & Schwartz 1989; Madejski et al. 1992), for these observations we investigated whether a broken power law could be consistent with the LE + ME data. We used an absorbed broken power law for the form $dN/dE \propto \exp[-N_H \sigma(E)]E^{-\alpha_1}$ for $E \leq E_0$, $dN/dE \propto E^{-\alpha_2}$ for $E \geq E_0$. Because of the limited statistics of our data, we fitted the spectra by fixing N_H and the break energy E_0 and allowing only three parameters to vary (α_1, α_2, and the normalization). We repeated the fit varying E_0 in the range permitted by the data coverage.

TABLE 3

MODEL RESULTS

OBJECT (1)	$F_{2-6\ keV}$ ($\times 10^{-12}$ ergs cm^{-2} s^{-1}) (2)	ME: N_H FIXED		LE + ME: N_H FIXED		LE + ME: N_H FREE		
		α (3)	χ^2_r/dof (4)	α (5)	χ^2_r/dof (6)	α (7)	N_H ($\times 10^{20}$ cm^{-2}) (8)	χ^2_r/dof (9)
H0323+022: N_H(Gal) = 8.4 × 10^{20} cm^{-2}								
1984 Sep 21	4.3	$2.81^{+0.34}_{-0.31}$	0.72/16	2.73 ± 0.10	0.67/19	$2.83^{+0.30}_{-0.27}$	$10^{+6.0}_{-9.9}$	0.70/18
1984 Sep 23	6.5	2.45 ± 0.30	0.64/13	2.37 ± 0.09	0.78/14	2.46 ± 0.36	$9.9^{+7.3}_{-5.0}$	8.83/13
H0414+009: N_H(Gal) = 8.6 × 10^{20} cm^{-2}								
1984 Sep 9	16.2	1.90 ± 0.10	1.07/25	1.94 ± 0.07	1.03/28	1.91 ± 0.11	$7.4^{+3.7}_{-2.3}$	1.06/27
1984 Sep 14	18.9	1.89 ± 0.09	0.73/30	1.90 ± 0.08	0.9/32	1.89 ± 0.09	$7.7^{+2.3}_{-2.1}$	0.7/31
1984 Sep 22	12.0	2.34 ± 0.16	0.73/21	2.15 ± 0.07	1.00/23	2.36 ± 0.18	14.0 ± 5.0	0.83/22
1984 Sep 30	9.3	2.49 ± 0.20	0.94/21	2.34 ± 0.08	1.05/24	2.42 ± 0.21	$10.2^{+5.8}_{-4.0}$	1.07/23
H1426+428: N_H(Gal) = 1.4 × 10^{20} cm^{-2}								
1985 Jan 12	34.7	2.10 ± 0.07	0.80/25	2.06 ± 0.02	0.80/26	2.10 ± 0.07	1.8 ± 0.3	0.80/25
1985 Feb 24	33.6	2.08 ± 0.10	0.70/25	1.95 ± 0.03	1.30/28	1.98 ± 0.09	$1.5^{+0.5}_{-0.4}$	1.34/27
H1722+119: N_H(Gal) = 8.6 × 10^{20} cm^{-2}								
1985 Sep 3	6.1	2.65 ± 0.25	0.74/18	2.35 ± 0.09	1.10/21	$2.44^{+0.26}_{-0.24}$	$11.0^{+7.0}_{-4.0}$	1.13/20

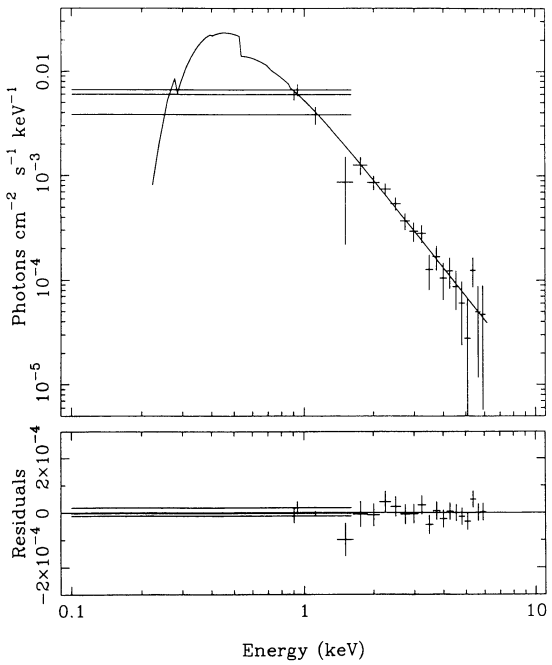

FIG. 1.—The 1984 September 21 LE + ME spectrum of H0323+022. *Upper panel*: the data deconvolved with a power law with free N_H. *Lower panel*: the residuals from this fit.

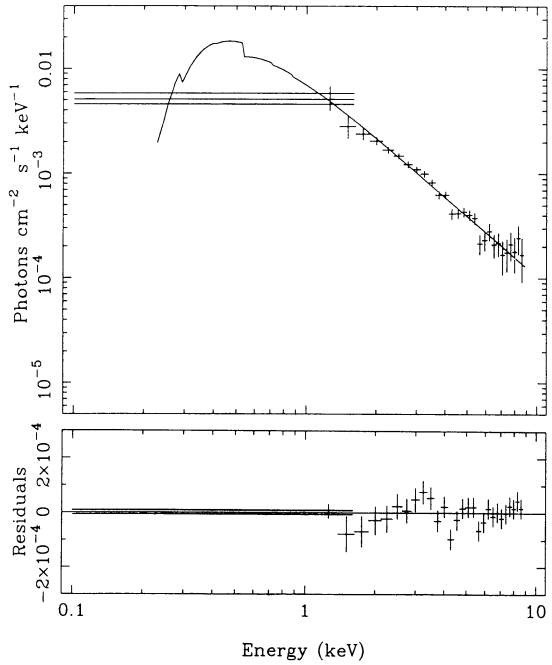

FIG. 3.—The 1984 September 9 LE + ME spectrum of H0414+009. Panels as in Fig. 1.

In the following sections we discuss the results for individual objects and compare them with those found from the previous missions.

5. INDIVIDUAL RESULTS

5.1. *H0323+022*

The source was observed with the *EXOSAT* satellite at seven epochs. Of these, only two observations (1984 September 21 and 23) satisfied the selection criteria described above (§ 3.1), having a signal significance above the 5 σ level and quality factor (QF) = 3. However, both spectra needed to be reextracted because of further technical problems, yielding improved results.

Signal from the source was detected in the energy range 0.1–6 keV. The results of the fits to the data are listed in Table 3. There is indication that the spectral index varied between the

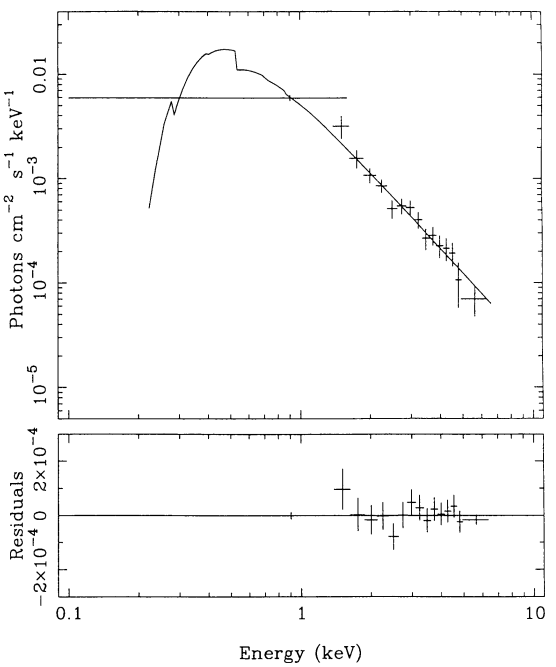

FIG. 2.—The 1984 September 23 LE + ME spectrum of H0323+022. Panels as in Fig. 1.

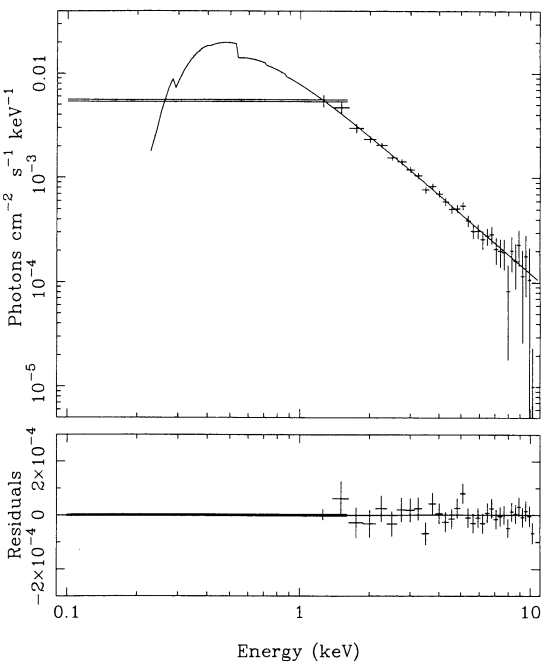

FIG. 4.—The 1984 September 14 LE + ME spectrum of H0414+009. Panels as in Fig. 1.

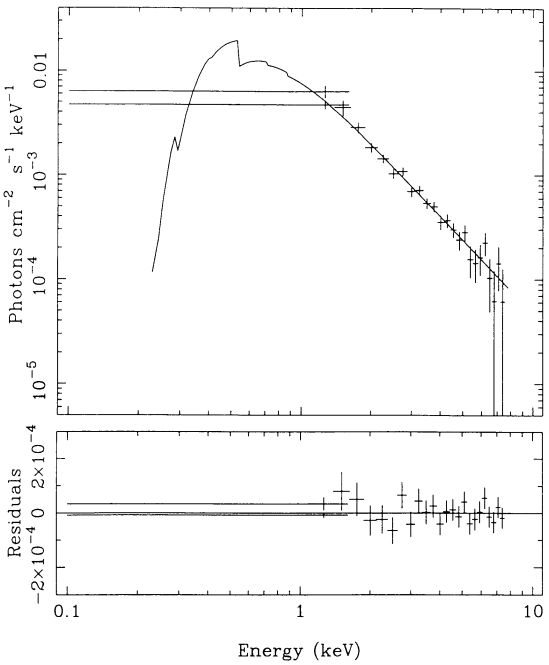

FIG. 5.—The 1984 September 22 LE + ME spectrum of H0414+009. Panels as in Fig. 1.

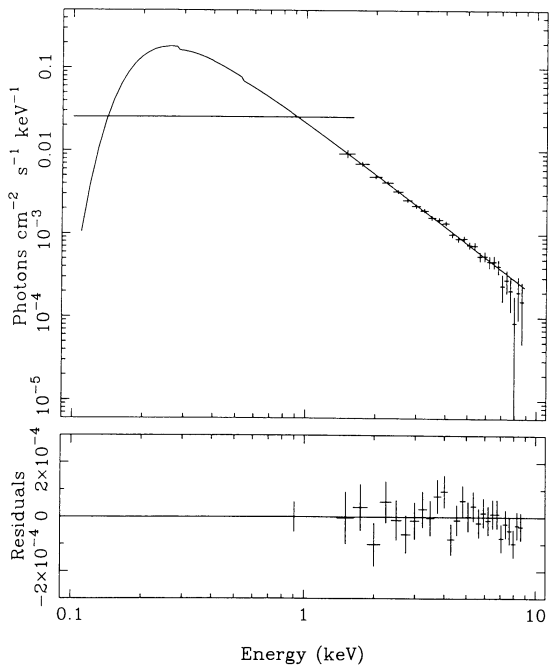

FIG. 7.—The 1985 January 12 LE + ME spectrum of H1426+428. Panels as in Fig. 1.

two observations, being ~2.6–2.8 on September 21 and lower (~2.4–2.5) on September 23. In particular, the September 21 slope is the highest found here. The change is in the sense of a hardening of the spectrum when the source brightens, as is apparent from Table 3. A similar, more pronounced trend was also found in the *Ginga* data (Table 1). In the *EXOSAT* data the intensity change is apparent only in the ME range. At soft energies the source remains essentially constant (Table 2).

It is interesting to note that the *Einstein* observations (Table 1), which covered an energy range similar to that of the *EXOSAT* ones, are consistent with a two-component spectrum. The slope of the IPC data is flatter than that of the simultaneous MPC data, and the absorbing column density is greater than the Galactic value. This suggested to Madejski & Schwartz (1989) a steepening of the spectrum above 1–3 keV. In the *EXOSAT* data, no evidence for a spectral break is

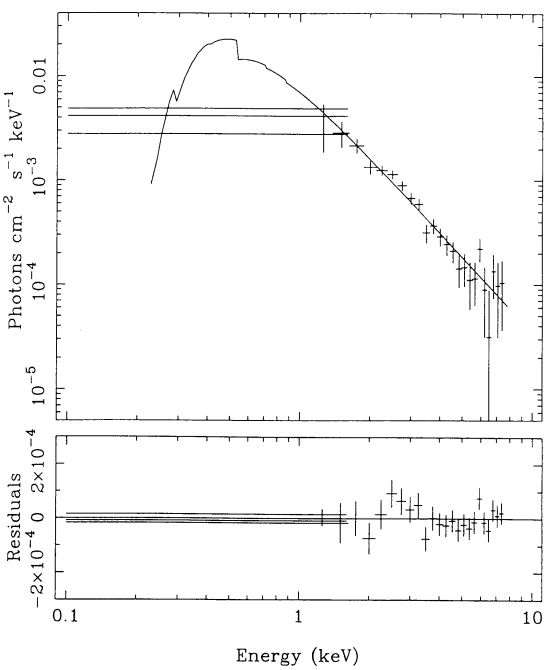

FIG. 6.—The 1984 September 30 LE + ME spectrum of H0414+009. Panels as in Fig. 1.

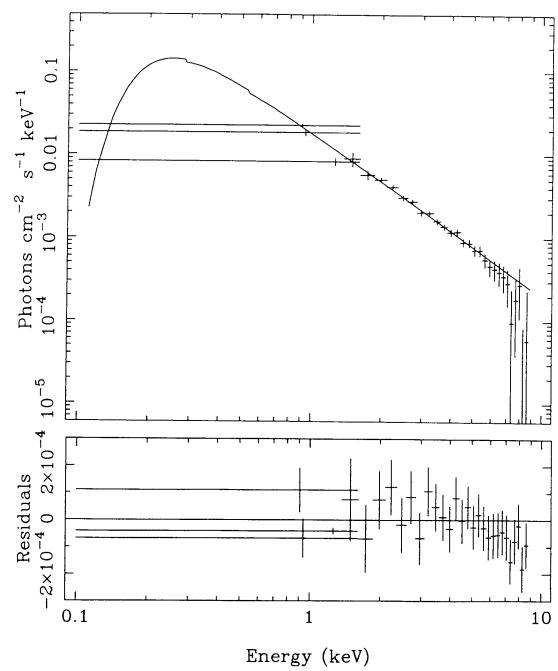

FIG. 8.—The 1985 February 24 LE + ME spectrum of H1426+428. Panels as in Fig. 1.

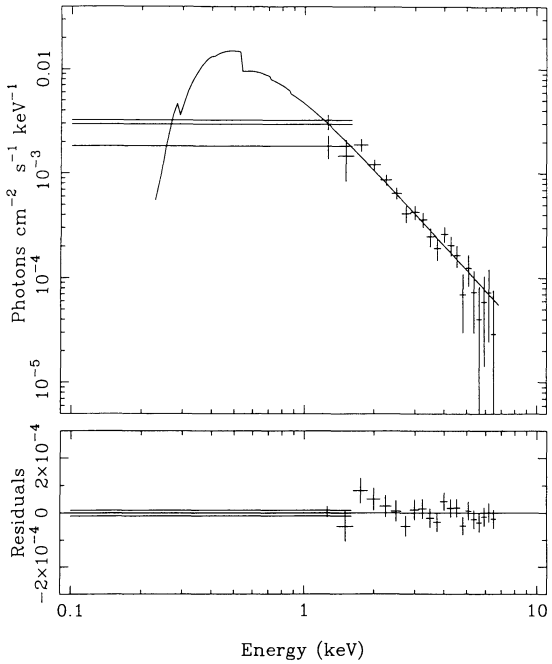

FIG. 9.—The 1985 September 3 LE + ME spectrum of H1722+119. Panels as in Fig. 1.

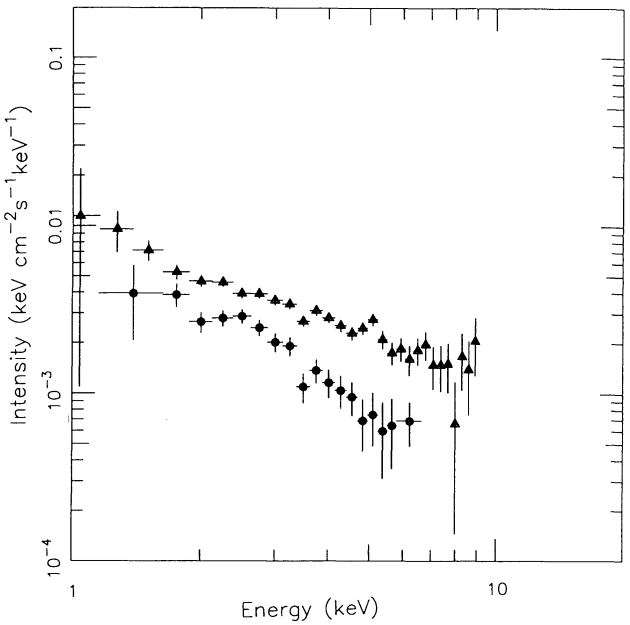

FIG. 10.—Comparison between the high state (*triangles*) of 1984 September 14 and the low state (*circles*) of 1984 September 30 for H0414+009.

present, the indexes of the ME data alone (col. [3]) and of the LE + ME data (col. [5]) being consistent within the errors, and N_H (col. [8]) in agreement with the Galactic value.

We conclude that the *EXOSAT* spectrum of H0232+022 can be described with a single–power-law model. The spectral slope seems to vary with the intensity, in such a way that the spectrum hardens when the source brightens.

5.2. *H0414+009*

EXOSAT observed H0414+009 on four occasions close in time (1984 September; see Table 2). In all cases but one (September 22) the quality of the spectrum was high. We retrieved the high-quality observations from the data base and reextracted the September 22 spectrum. A previous spectral study on the *EXOSAT* data was done in an unpublished work by George (1988), while diffuse emission was searched for by McHardy et al. (1992).

The source was detected up to ~8 keV. On one occasion (September 30), a positive signal was detected up to ~10 keV. The spectral analysis results are shown in Table 3. The spectral slope is variable, ranging from ~1.8 on September 14, which is the lowest value in Table 3, to ~2.4 on September 30. The 2–6 keV flux ranges from $\sim 19.0 \times 10^{-12}$ ergs cm^{-2} s^{-1} on September 14 to $\sim 9.0 \times 10^{-12}$ ergs cm^{-2} s^{-1} on September 30. As in the case of H0323+022 (§ 5.1), the spectral change is in the sense of a hardening when the source brightens. For H0414+009, owing to the greater number of observations and to the better quality of the data, the correlation is more reliable than for H0323+022. As an example, we plot in Figure 10 the high state (September 14) and the low state (September 30) data. A steepening of the spectrum when the source is in the low state is apparent.

A remarkable result of the analysis of the *Einstein* data (Table 1) was that an absorption column density in excess to the Galactic value was found. The extra absorption was convincingly attributed to highly ionized gas, intrinsic to the BL Lac object. It was found that a neutral absorber does not adequately reproduce the X-ray spectrum, and that instead a model including an absorption line between 0.5 and 0.6 keV, possibly due to ionized oxygen (Canizares & Kruper 1984; Madejski et al. 1991), did improve the fit. We checked whether the enclosure of a feature at 0.6 keV would be consistent with both low-state spectra, but we did not find convincing results in either case. However, the lack of spectral resolution in our data below ~1 keV does not allow us to exclude the presence of a feature in the soft energy range.

In summary, the *EXOSAT* spectrum of H0414+009 is well represented by a single power law over the energy range 0.2–10 keV. Apparently the intensity and the slope are correlated, the spectrum becoming harder when the source brightens.

5.3. *H1426+428*

H1426+28 was observed twice with the *EXOSAT* satellite, on 1985 January 12 and February 24. Both these observations satisfied the 5 σ detection criterion, but only the first spectrum had an acceptable QF. This spectrum was previously studied by Remillard et al. (1989). In the second case, the low quality of the archival spectrum could be attributed to the fact that during the observation only three detectors were on, requiring a more accurate background subtraction. The rextraction gave higher quality data.

The signal from the source covers the range from 0.1 to ~8–9 keV. The spectral analysis results are shown in Table 3. For both observations we obtained very close indexes for all the fits, without evidence for curvature. The source did not change in intensity or in spectral shape between the two observing epochs. Because of this, to improve the statistic, we fitted the 12 January and the 24 February spectra together. We obtained $\alpha = 2.03 \pm 0.05$ and $N_H = (1.6 \pm 0.3) \times 10^{20}$ cm^{-2},

in excellent agreement with the Galactic value (1.4×10^{20} cm^{-2}). It is remarkable that the slope found for H1426+428 is one of the flattest in Table 3. This is consistent with the findings by Fink et al. (1992) in the soft energy range 0.1–2.4 keV, in a preliminary report of the *ROSAT* observations for a sample of 10 bright BL Lac objects. They give for H1426+428 a spectral index of 2.10 ± 0.10, while the average for the entire sample was 2.39 ± 0.07.

Recently, Madejski et al. (1992) published a preliminary description of the BBXRT spectrum of H1426+428. They found that the data require an absorption feature at $\sim$0.6 keV and a spectral break with a steepening of $\Delta\alpha \sim 0.7$ at $\sim$1.5–2.0 keV. The 0.6 keV feature is similar to that discovered in PKS 2155−304 by Canizares & Kruper (1984) and in a few other BL Lac objects by Madejski et al. (1991) in the *Einstein* data. It is interpreted as an O VIII resonant line.

With reference to the line, the fact that no excess N_H is required does not cause us to suspect a priori the presence of a feature at low energies. However, we cannot exclude its presence because of the lack of resolution below 1 keV in our data.

As can be seen in Figures 7 and 8 (*upper panels*), a systematic downward trend above $\sim$5 keV is present in both spectra, which is more pronounced in the February 24 observation. Although the error bars of the data points are large, the residuals (*lower panels*) show that the fit is poorer at higher energies. We checked whether the data could be consistent with a broken power law. A fit to the spectra with this model, in the way described in § 4, indicated a steepening at $E_0 \sim 5$ keV, with $\alpha_1 \sim 2.00$ and $\alpha_2 \sim 3.00$ in both cases. The quality of the fit improved by $\Delta\chi^2 = 5.3$ and $\Delta\chi^2 = 11$ in the January 12 and February 24 data, respectively. The improvement is significant only in the second case (at $\sim$95% with the *F*-test) and is more evident if we fit the two spectra together. In fact, this yielded $\Delta\chi^2 = 16.7$ with a significance greater than 99.9%.

In summary, in the *EXOSAT* spectra rather well-defined evidence for curvature at higher energies is found. The spectra are among the flattest known for X-ray–selected BL Lac objects.

5.4. *H1722+119*

This object was observed only once by *EXOSAT*, at a relatively bright emission level (Table 2). The count rates of the source are comparable to the low state of H0323+022, both in the LE and the ME bands. The good quality of the spectrum (QF = 4) allowed us to retrieve it from the data base and to perform a spectral study. Signal was found in the range 0.1–6 keV. The power-law fit is acceptable, and no indication for curvature is present.

6. DISCUSSION AND CONCLUSIONS

In this paper we present new results from *EXOSAT* for a group of four X-ray–selected BL Lac objects. We modeled the 0.1–10 keV energy distributions with a single power law, corrected for absorption by cold gas. Two sources (H0323+022 and H0414+009), for which more than one observation was available, exhibit spectral variability in the sense of a hardening of the spectrum when the source brightens. No presence of curvature was detected significantly in the *EXOSAT* data, except for H1426+428, where a steepening at higher energies (>5 keV) is found.

Our results integrate and support the observational framework established by previous investigations. Although our sample includes only four sources (nine observations in total), it can be interesting to compare the X-ray average slope to that of other active galaxtic nuclei (AGNs). From the fits with a power law with fixed N_H, averaging the values in column (5) we derive $\langle\alpha\rangle = 2.20$ with standard deviation 0.26, and a total reduced χ^2 of 0.84 for 215 dof, indicating that for all the objects as a class the single–power-law model with low energy absorption due solely to interstellar matter gives satisfactory fits. This supports the proposal that BL Lac objects are steeper than other classes of AGNs (Turner & Pounds 1989; Canizares & White 1989; Wilkes & Elvis 1987; Lawson et al. 1992) and, among blazars, steeper than the class of highly polarized quasars (Worrall & Wilkes 1990). In particular, X-ray–selected BL Lac objects are found to have greater X-ray slopes than radio-selected ones (Worrall & Wilkes 1990).

Spectral variability, in the sense reported above, was noted in the *EXOSAT* observations of a sample of BL Lac objects by Giommi et al. (1990). By plotting the ME/LE count-rate ratio against the ME intensity for the six brightest sources of their sample, an increase of the hardness ratio with intensity was observed, implying that the sources' spectra harden as their fluxes increase. This trend was also detected by a spectral analysis for some individual sources (George, Warwick, & Bromage 1988a; George, Warwick, & McHardy 1988b; Treves et al. 1989). However, this picture was not always supported by the data collected by other X-ray missions in nearby or overlapping energy bands. For example, PKS 2155−304 and Mrk 421 were observed by the *Ginga* satellite to vary dramatically in intensity in the range 2–35 keV without spectral change (Ohashi 1989; Ohashi et al. 1989), and the *ROSAT* observations of Mrk 421 in the range 0.2–2.4 keV detected a flattening with fading intensity (Fink et al. 1991). Our results for H0323+022 and H0414+009 confirm the trend discovered by Giommi et al. (1990), increasing the number of individual sources for which it is observed.

In a cumulative study of the *EXOSAT* data for a sample of 17 BL Lac objects, in the energy range 0.1–10 keV, Barr et al. (1989) preliminarily reported a global steepening of the spectra at lower energies, consistent with the findings of Madejski & Schwartz (1989), who analyzed the simultaneous *Einstein* IPC and MPC data for six sources. A convexity was also detected in the spectra of a few isolated cases. The spectrum of Mrk 421 during an outburst is better modeled by adding a high-energy cutoff to a single–power-law model (George et al. 1988b); PKS 0548−322 shows a convex spectrum in two cases (Barr et al. 1988; Garilli & Maccagni 1990), with breaks at 5 and 2 keV, respectively. In our data, the only significant (at the 95% confidence level) indication for a break in the spectrum was detected for H1426+428, where a steepening occurs above 5 keV. It is interesting to note also that the BBXRT data for this object were consistent with a broken power law (Madejski et al. 1992), but the break point was found at lower energies (2–3 keV). A similar feature is present for PKS 0548−322, for which the break point was found to move to lower energies when the source brightens (Garilli & Maccagni 1990). Unfortunately, because the intensity of H1426+428 at the time of the BBRXT observations is not known, we cannot comment further on this behavior.

In conclusion, the new *EXOSAT* data presented here for four X-ray–selected BL Lac objects support the observational framework established up to now. In particular, the spectral variability of the BL Lac objects is confirmed, as a distinguishing feature of this class among AGNs.

REFERENCES

Barr, P., Giommi, P., & Maccagni, D. 1988, ApJ, 324, L11
Barr, P., Giommi, P., Pollock, A., Tagliaferri, G., Maccagni, D., & Garilli, B. 1989, in BL Lac Objects, ed. L. Maraschi, T. Maccaro, & M.-H. Ulrich (Berlin: Springer-Verlag), 267
Brissenden, R. J. V., Remillard, R. A., Tuohy, I. R., Schwartz, D. A., & Hertz, P. L. 1990, ApJ, 350, 578
Canizares, C. R., & Kruper, J. 1984, ApJ, 278, L99
Canizares, C. R., & White, J. L. 1989, ApJ, 339, 27
de Korte, P. A. J., et al. 1981, Spa. Sci. Rev., 30, 495
Doxsey, R., Bradt, H., McClintock, J., Petro, L., Remillard, R., Ricker, G., Schwartz, D., & Wood, K. 1983, ApJ, 264, L43
Elvis, M., Lochmann, F. J., & Wilkes, B. 1989, AJ, 97, 777
EXOSAT Database System: Available Databases. 1991, ed. C. Barron ESA TM-13
Feigelson, E. D., et al. 1986, ApJ, 302, 337
Filippenko, A. V., Djorgovski, S., Spinrad, H., & Sargent, W. L. W. 1986, AJ, 91, 49
Fink, H. H., Thomas, H.-C., Brinkmann, W., Okayasu, R., & Hartner, G. 1992, MPE Rep. 235 (Garching: MPI), 202
Fink, H. H., Thomas, H.-C., Hasinger, G., Predehl, P., Schaeidt, S., Makino, F., & Warwick, R. S. 1991, A&A, 246, L6
Garilli, B., & Maccagni, D. 1990, A&A, 229, 88
George, I. M. 1988, Ph.D. thesis, Univ. Leicester
George, I. M., Warwick, R. S., & Bromage, G. E. 1988a, MNRAS, 232, 793
George, I. M., Warwick, R. S., & McHardy, I. M. 1988b, MNRAS, 235, 787
Giommi, P., Barr, P., Garilli, B., Maccagni, D., & Pollock, A. 1990, ApJ, 356, 432
Giommi, P., & Tagliaferri, G. 1991, XIMAGE User's Guide, Version 1.8 (Noordwijk: ESA)
Griffiths, R. E., Wilson, A. S., Ward, M. J., Tapia, S., & Ulvestad, J. S. 1989, MNRAS, 240, 33
Halpern, J., Chen, V. S., Madejski, G. M., & Chanan, G. A. 1991, AJ, 101, 818
Lawson, A. J., Turner, M. J. L., Williams, O. R., Stewart, G. C., & Saxton, R. D. 1992, MNRAS, in press
Madejski, G. M. 1985, Ph.D. thesis, Harvard Univ.
Madejski, G. M., & Schwartz, D. A. 1989, in BL Lac Objects, ed. L. Maraschi, T. Maccacaro, & M.-H. Ulrich (Berlin: Springer-Verlag), 267
Madejski, G. M., et al. 1992, in Proc. 28th Yamada Conf. on Frontiers of X-Ray Astronomy, ed. Y. Tanaka & K. Koyama (Tokyo: Universal Academy Press), 583
Madejski, G. M., Mushotzky, R. F., Weaver, K. A., Arnaud, K. A., & Urry, C. M. 1991, ApJ, 370, 198
Maraschi, L., & Maccagni, D. 1988, Mem. Soc. Astron. Italiana, 59, 277
McHardy, I. M., Luppino, G. A., George, I. M., Abraham, R. G., & Cooke, B. A. 1992, MNRAS, 256, 655
Morrison, R., & McCammon, D. 1983, ApJ, 270, 119
Ohashi, T. 1989, in BL Lac Objects, ed. L. Maraschi, T. Maccacaro, & M.-H. Ulrich (Berlin: Springer-Verlag), 296
Ohashi, T., Makishima, K., Inoue, H., Koyama, K., Makino, F., Turner, M. J. L., & Warwick, R. S. 1989, PASJ, 41, 709
Piccinotti, G., Mushotzky, R. F., Boldt, E. A., Holt, S. S., Marshall, F. E., Serlemitsos, P. J., & Shafer, R. A. 1982, ApJ, 253, 485
Remillard, R. A., Tuohy, I. R., Brissenden, R. J. V., Buckley, D. A. H., Schwartz, D. A., & Tapa, S. 1989, ApJ, 345, 140
Shafer, R. A., Haberl, F., Arnaud, K. A., & Tennant, A. F. 1991, XSPEC User's Guide, Version 2 (ESA TM-09)
Stark, A. A., Gammie, C. F., Wilson, R. W., Bally, J., Linke, R. A., Heiles, C., & Hurwitz, M. 1992, ApJS, 79, 77
Treves, A., et a 1989, ApJ, 341, 733
Turner, M. J. L., Smith, A., & Zimmermann, H. V. 1981, Spa. Sci. Rev., 30, 513
Turner, T. J., & Pounds, K. A. 1989, MNRAS, 240, 833
Ulmer, M. P., Brown, R. L., Schwartz, D. A., Patterson, J., & Cruddace, R. G. 1983, ApJ, 270, L1
Urry, C. M. 1986, in Continuum Emission in AGN, ed. M. L. Sitko (Tucson: NOAO), 91
Wilkes, B., & Elvis, M. 1987, ApJ, 323, 243
Worrall, D. M. & Wilkes, B. J. 1990, ApJ, 360, 296